Electronic Supplementary Material (ESI) for Journal of Materials Chemistry A.

Supporting Information

Regulation of a Ni_3Sn_2 intermetallic catalyst using highly dispersed Pd species to boost propyne semi-hydrogenation

Kelin Yan,[a] Xiaohu Ge,[*a] Wenhua Li,[a] Yijing Liang,[a] Weijian Xiong,[a] Jing Zhang,[a] Gang Qian,[a] De Chen,[b] Yueqiang Cao,[*a] Xinggui Zhou,[a] Xuezhi Duan[a]

[a] *State Key Laboratory of Chemical Engineering, School of Chemical Engineering, East China University of Science and Technology, Shanghai 200237, China*

[b] *Department of Chemical Engineering, Norwegian University of Science and Technology, Trondheim 7491, Norway*

**Corresponding Author: xhge@ecust.edu.cn; yqcao@ecust.edu.cn*

Table S1. Composition of the Ni_3Sn_2, $(Ni_{0.9}Pd_{0.1})_3Sn_2$ and $(Ni_{0.8}Pd_{0.2})_3Sn_2$ catalysts.

Samples	Ni loading (wt%)[a]	Sn loading (wt%)[a]	Pd loading (wt%)[a]	Ni/Pd atomic ratio
Ni_3Sn_2	9.92	10.74	/	/
$(Ni_{0.9}Pd_{0.1})_3Sn_2$	7.46	9.94	1.55	8.65
$(Ni_{0.8}Pd_{0.2})_3Sn_2$	7.21	7.88	3.00	4.32

[a] Determined by ICP-AES.

Table S2. Adsorption configurations and energies of propyne on Ni_3Sn_2 catalyst.

Top view	Side view	E_{ads} (eV)
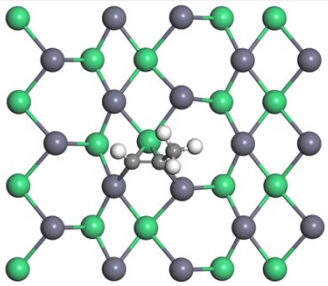	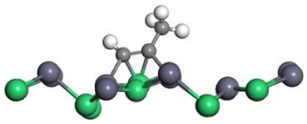	-0.92
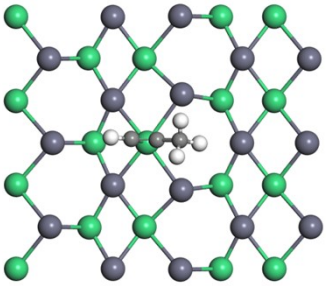	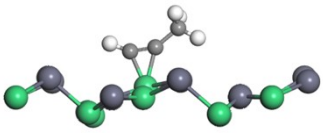	-0.50
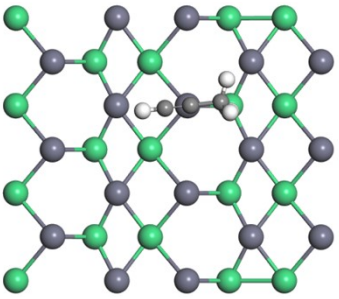	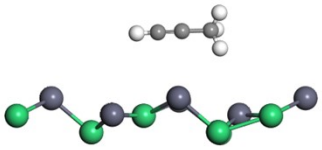	-0.14

Table S3. Adsorption configurations and energies of propyne on $(Ni_{0.9}Pd_{0.1})_3Sn_2$ catalyst.

Top view	Side view	E_{ads} (eV)
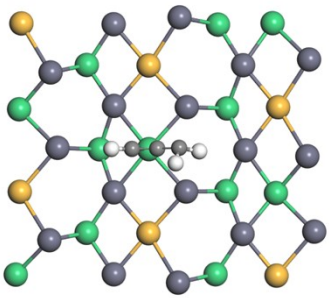	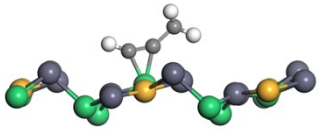	-0.51
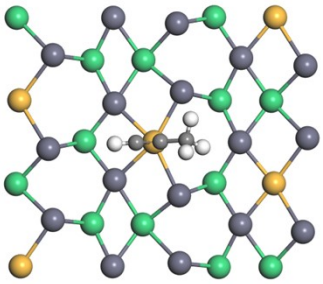	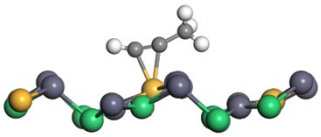	-0.43
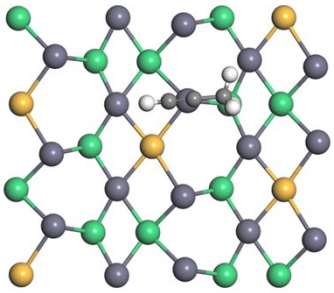	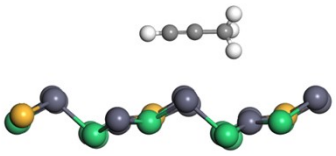	-0.20

Table S4. Adsorption configurations and energies of propyne and hydrogen atom on $(Ni_{0.9}Pd_{0.1})_3Sn_2$ catalyst.

Top view	Side view	E_{ads} (eV)
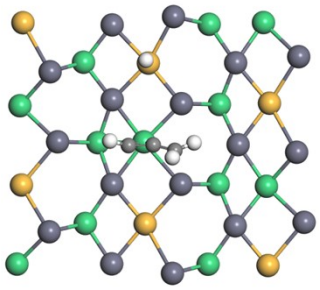	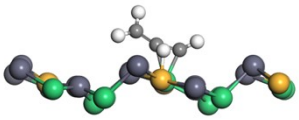	-0.65
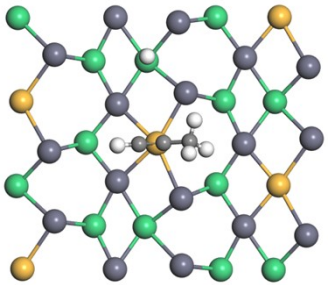	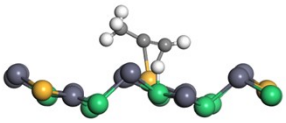	-0.52

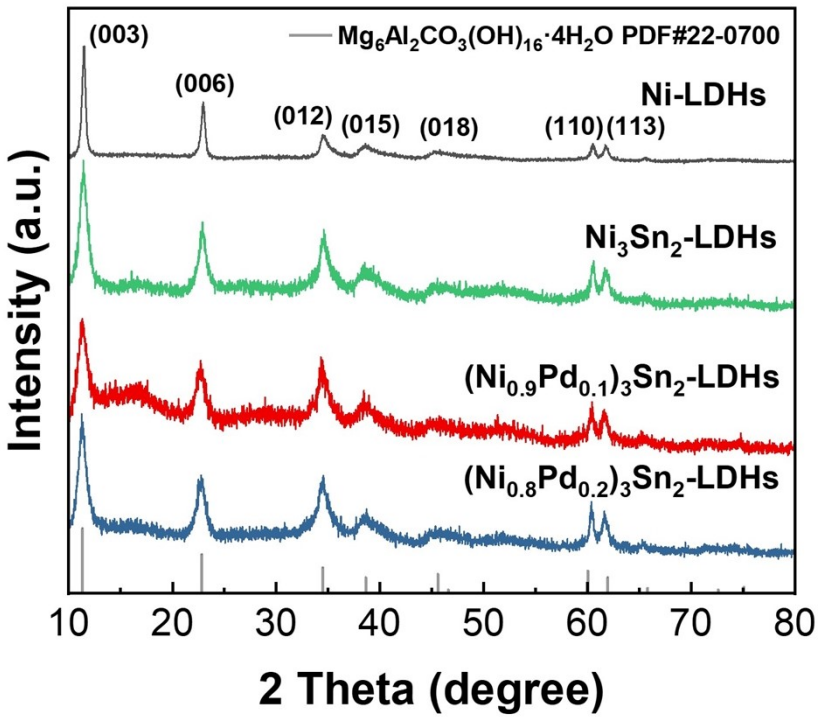

Fig. S1. XRD profiles of Ni-LDHs, Ni_3Sn_2-LDHs, $(Ni_{0.9}Pd_{0.1})_3Sn_2$-LDHs and $(Ni_{0.8}Pd_{0.2})_3Sn_2$-LDHs.

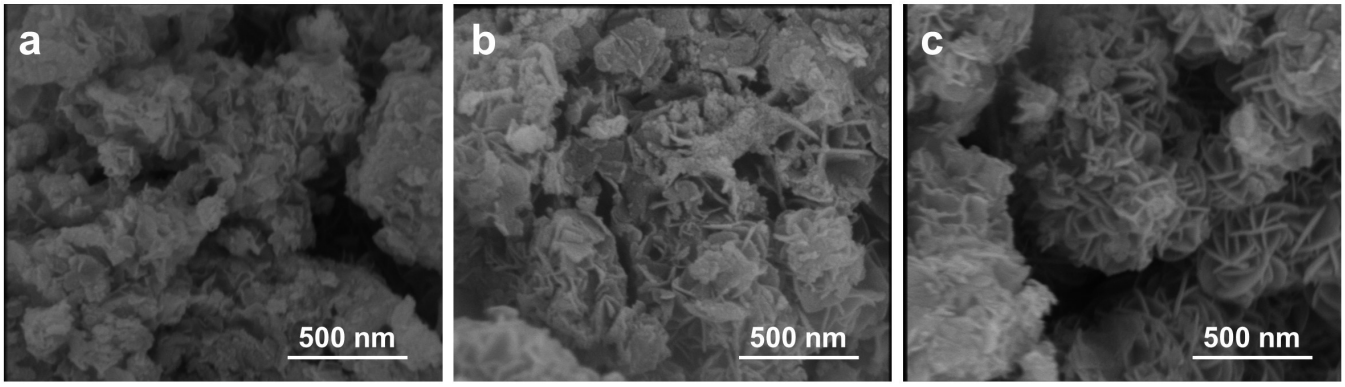

Fig. S2. Typical SEM images of (a) Ni_3Sn_2-LDHs, (b) $(Ni_{0.9}Pd_{0.1})_3Sn_2$-LDHs and (c) $(Ni_{0.8}Pd_{0.2})_3Sn_2$-LDHs.

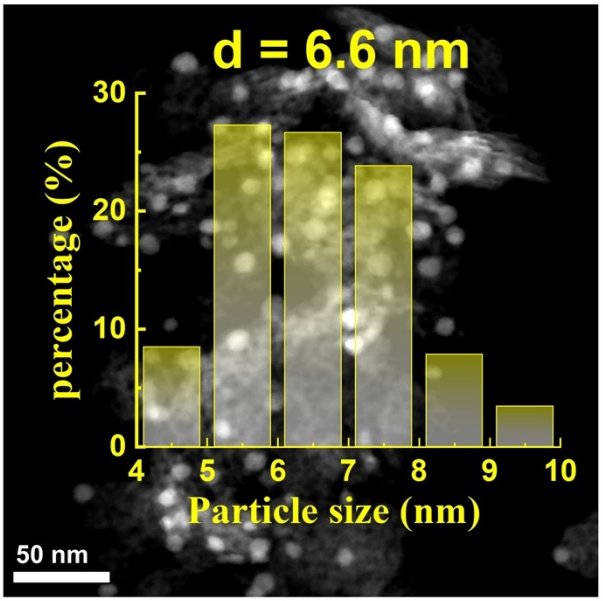

Fig. S3. HAADF-STEM images and corresponding histograms of the particle size distributions of Ni catalyst.

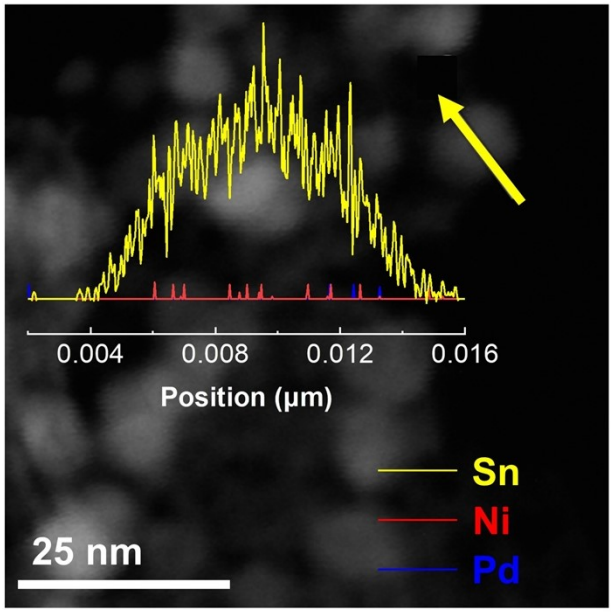

Fig. S4. HAADF-STEM EDS line-scanning profiles of Ni catalyst.

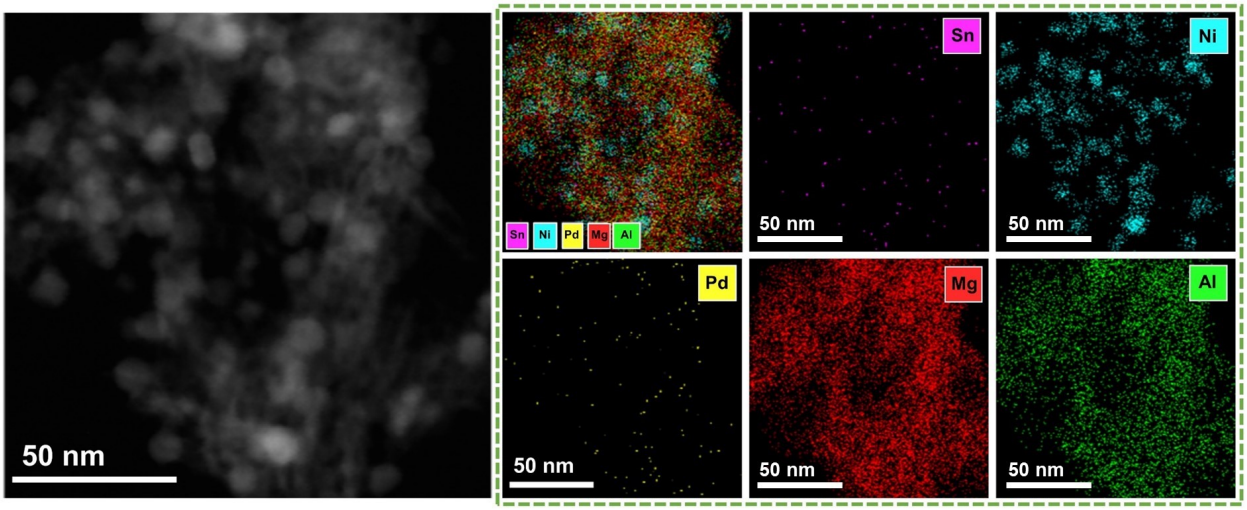

Fig. S5. HAADF-STEM EDS mapping analyses of Ni catalyst.

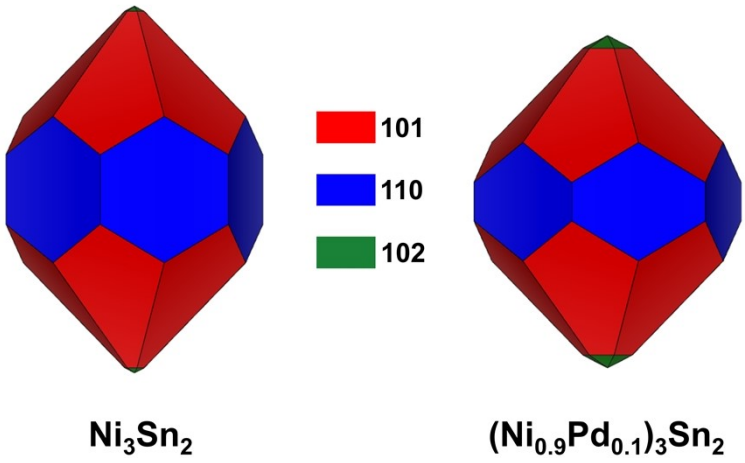

Fig. S6. Wulff crystals for Ni_3Sn_2 and $(Ni_{0.9}Pd_{0.1})_3Sn_2$ intermetallics, where the crystal facets by Miller indices are shown by different colors.

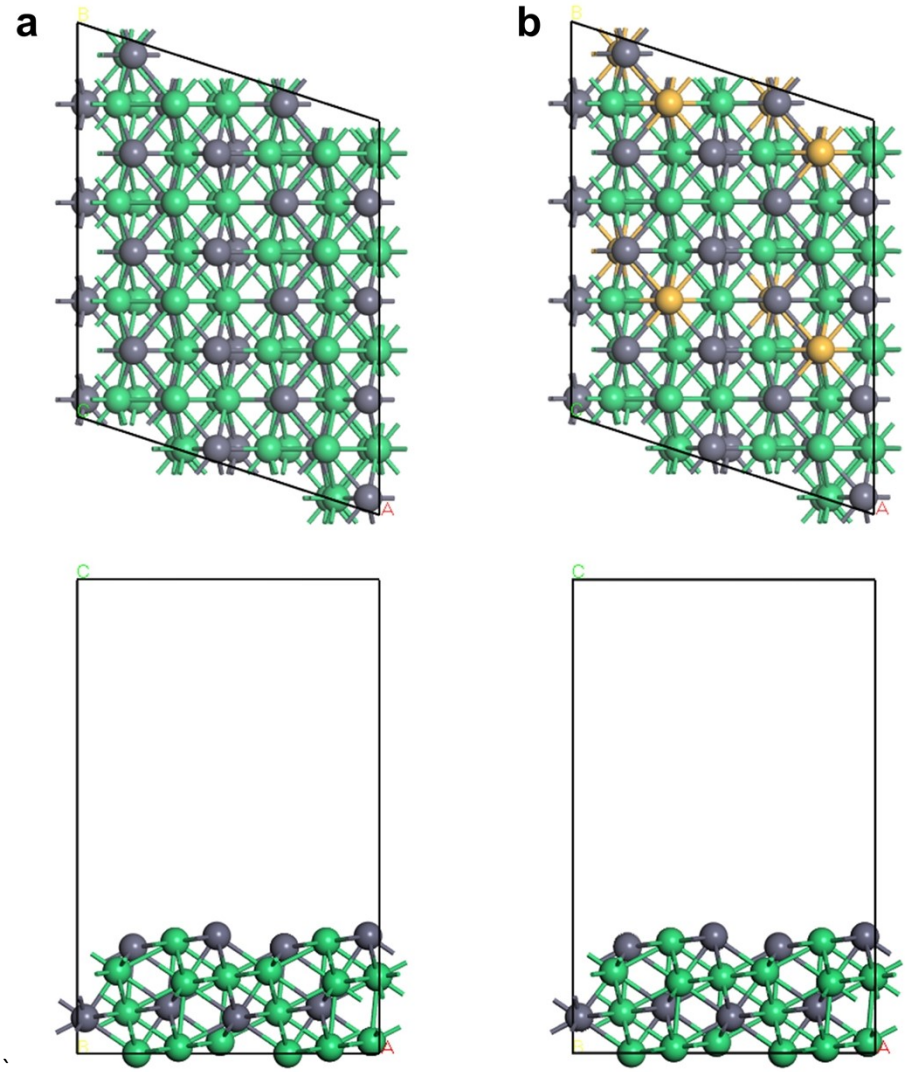

Fig. S7. Schematical illustrations of (a) $Ni_3Sn_2(101)$ and (b) $(Ni_{0.9}Pd_{0.1})_3Sn_2(101)$. The green, gray and yellow balls represent Ni, Sn and Pd atoms, respectively.

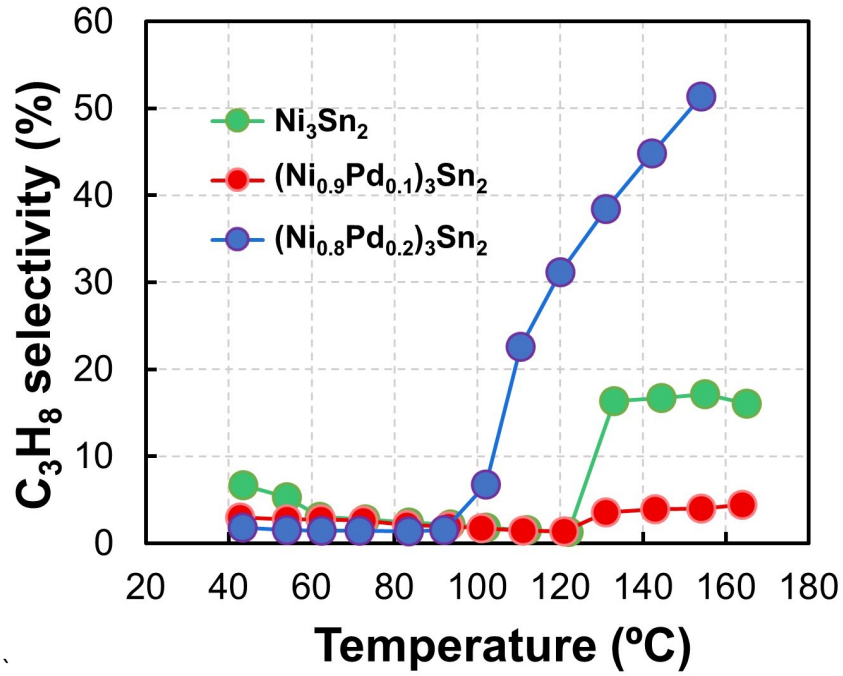

Fig. S8. Propane selectivity as a function of temperature over the Ni_3Sn_2, $(Ni_{0.9}Pd_{0.1})_3Sn_2$ and $(Ni_{0.8}Pd_{0.2})_3Sn_2$ catalysts.

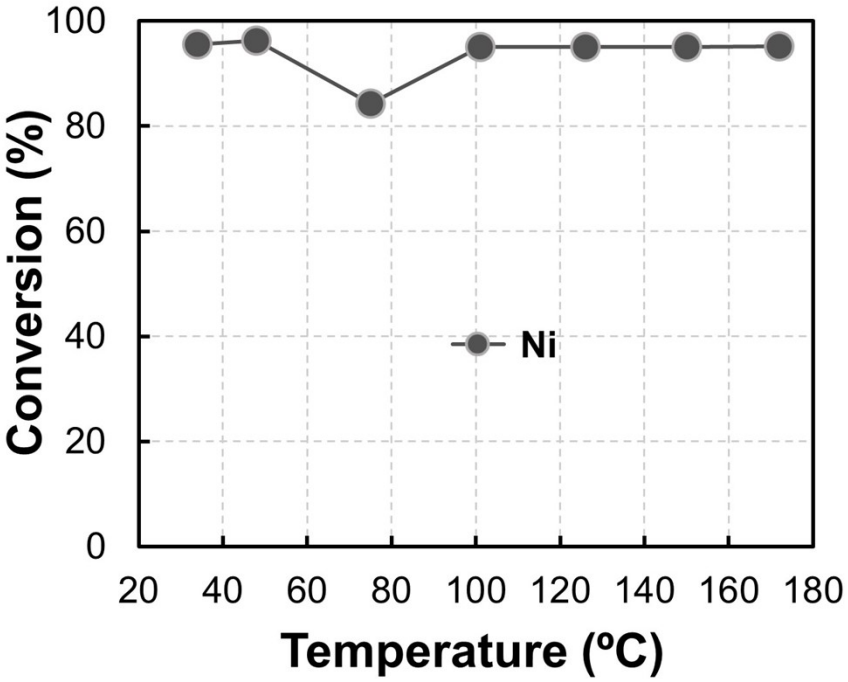

Fig. S9. Propyne conversion as a function of temperature over the Ni catalyst.

Fig. S10. Propylene selectivity as a function of temperature over the Ni catalyst.

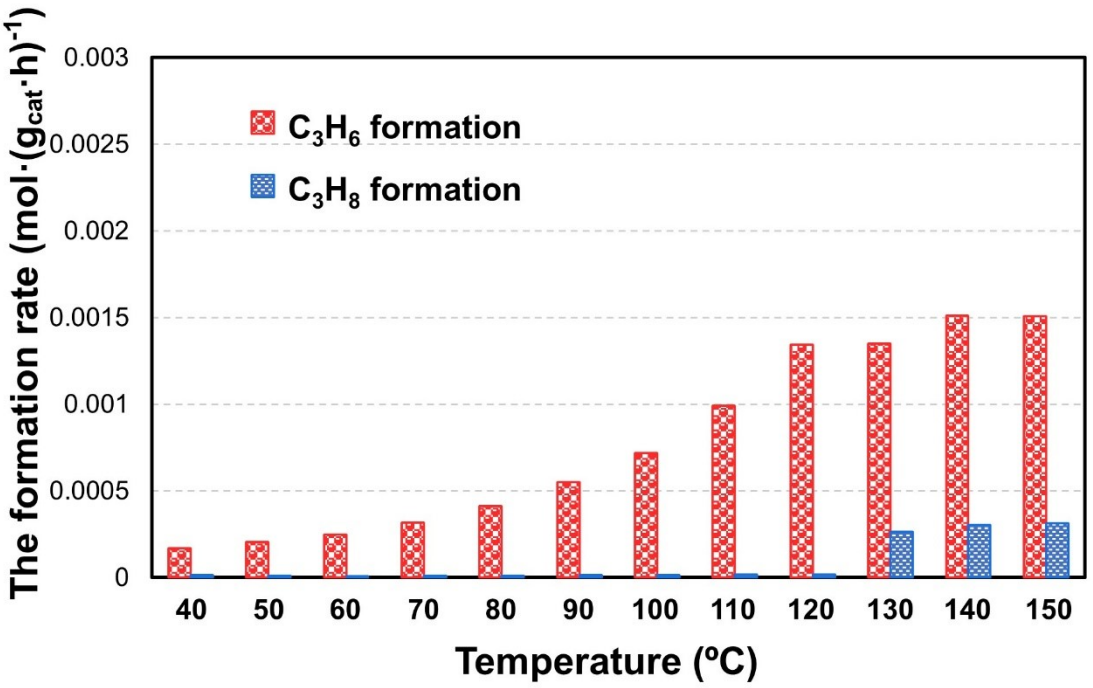

Fig. S11. The propylene and propane formation rate as a function of temperature over the Ni_3Sn_2 catalyst.

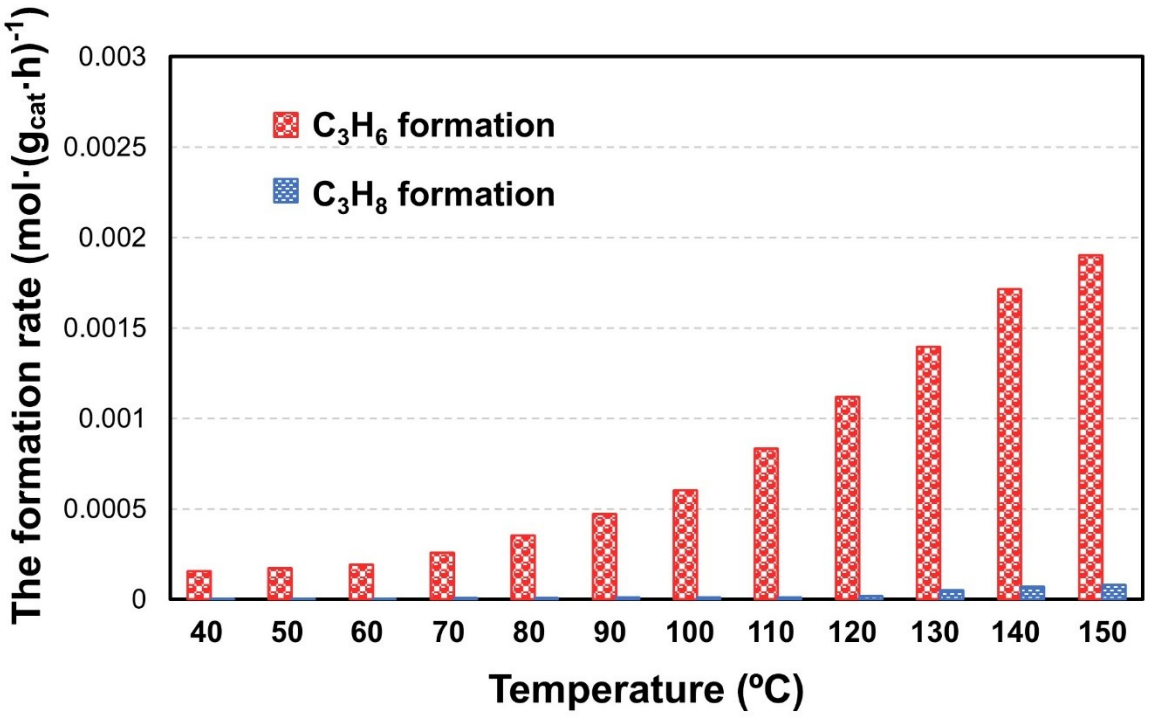

Fig. S12. The propylene and propane formation rate as a function of temperature over the $(Ni_{0.9}Pd_{0.1})_3Sn_2$ catalyst.

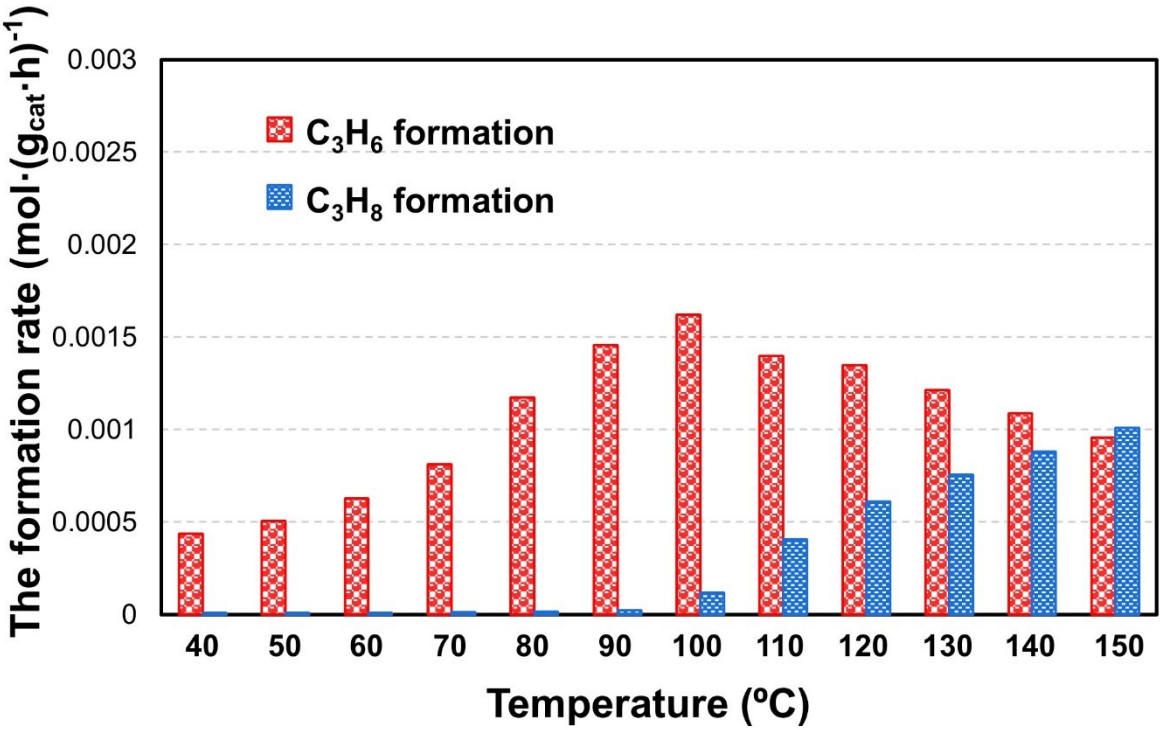

Fig. S13. The propylene and propane formation rate as a function of temperature over the $(Ni_{0.8}Pd_{0.2})_3Sn_2$ catalyst.

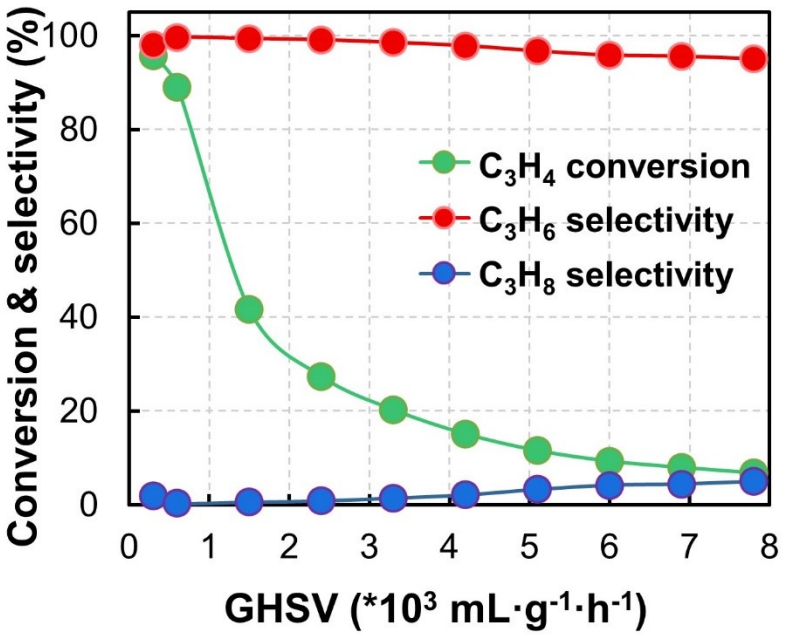

Fig. S14. Catalytic performance of the $(Ni_{0.9}Pd_{0.1})_3Sn_2$ catalyst under different space velocities.

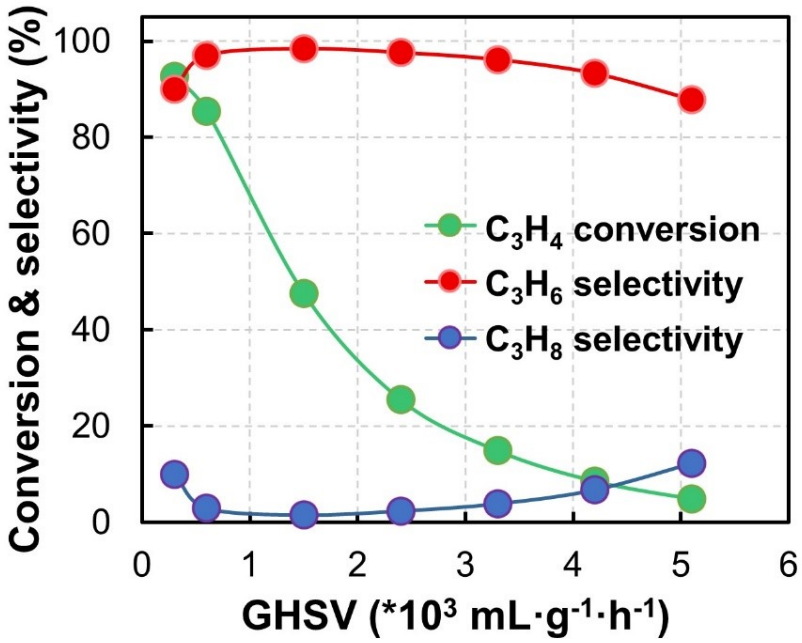

Fig. S15. Catalytic performance of the Ni_3Sn_2 catalyst under different space velocities.

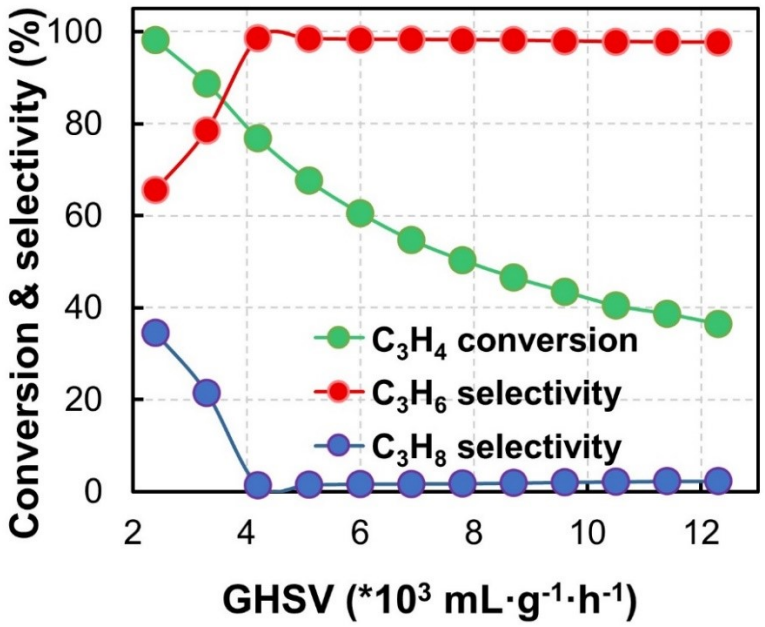

Fig. S16. Catalytic performance of the $(Ni_{0.8}Pd_{0.2})_3Sn_2$ catalyst under different space velocities.